

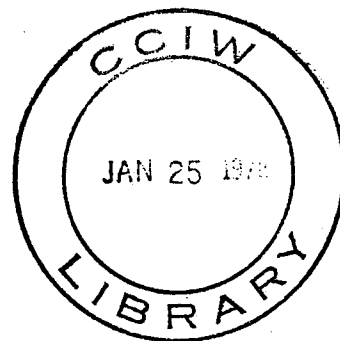


**Environment  
Canada**

**Environnement  
Canada**

**Canada  
Centre  
For Inland  
Waters**

**Centre  
Canadien  
Des Eaux  
Intérieures**



DETERMINATION OF BED-LOAD  
FROM MEASUREMENTS OF DUNE  
PROFILES - AN INTERIM REPORT

by  
P. Engel

**UNPUBLISHED REPORT  
RAPPORT NON PUBLIE**

TD  
7  
E54  
1977a

DETERMINATION OF BED-LOAD  
FROM MEASUREMENTS OF DUNE  
PROFILES - AN INTERIM REPORT

by  
P. Engel

Hydraulics Section  
Hydraulics Research Division  
Canada Centre for Inland Waters  
August 1977

## TABLE OF CONTENTS

	<u>Page</u>
SUMMARY	iii
1.0 INTRODUCTION	I
2.0 BED-LOAD EQUATIONS USING DATA FROM BED PROFILES	3
2.1 Theoretical Development	3
2.2 Determination of ( $\alpha k$ ) from Published Data	6
2.3 Variation of $K_{\Delta}$ with Flow Conditions	6
2.4 Summary of Data Analysis	8
2.5 Proposed Bed-load Equations Using Alternate Bedform Height	9
2.5.1 Equation using mean bed-form height	9
2.5.2 Equation using departures about mean bed elevation	9
3.0 EXPERIMENTAL EQUIPMENT	11
3.1 The Sediment Flume	11
3.2 Instruments	12
3.2.1 Bed level probe	12
3.2.2 Water level probe	12
3.2.3 Longitudinal (X-AXIS) displacement indicator	12
3.2.4 Analogue recorder	13
3.2.5 Timers	13
3.3 Sand	13
4.0 EXPERIMENTAL PROCEDURE AND PRELIMINARY DATA ANALYSIS	14
4.1 Initial Considerations	14
4.2 Initiations of Runs and Attainment of Equilibrium	14
4.3 Experimental Measurements	15
4.3.1 Measurement of profiles	15
4.3.2 Measurement of water discharge	15
4.3.3 Measurement of sediment discharge	16
4.4 Interpretation of Profiles	16
4.4.1 Water surface slope	16

4.4.2 Depth of flow	16
4.4.3 Bed-form speed	17
4.4.4 Bed-form heights	18
4.4.4.1 Mean bed-form height $\bar{\psi}$	18
4.4.4.2 Average departure about mean elevation $\bar{\epsilon}$	18
5.0 ANALYSIS OF THE PROPOSED BED-LOAD EQUATIONS	19
5.1 The $\bar{\psi}$ Equation	19
5.2 The $\bar{\epsilon}$ Equation	19
5.3 Comparison Between the Proposed Bed-load Equations and the Ackers - White Sediment Transport Formula	20
6.0 CONCLUSIONS	24
ACKNOWLEDGEMENT	
REFERENCES	
FIGURES	
TABLES	

## SUMMARY

An experimental study in a sediment flume was conducted to examine the usefulness of computing bed-load using bed-form height and speed obtained from sequences of profiles of the mobile bed taken a known length of time apart. A theoretical analysis was made to obtain a general bed-load equation for this purpose. This analysis showed that a coefficient was required to jointly take into account the geometry of the bed-form and that portion of the bed-form which contributes to bed-load transport. Dimensional analysis indicated that the coefficient should vary with flow conditions. Examination of published data, showed that such a coefficient varies strongly with mobility number and appears to be independent of depth for cases of practical interest.

The general bed-load equation was extended to two special cases for use with bottom profiles and tested. The first equation used a bed-form height  $\bar{\psi}$  obtained by dividing the volume per unit width of the bed-forms by their length. The second equation used the mean departure  $\bar{\epsilon}$  about the mean bed elevation as the characteristic bed-form height. The  $\bar{\epsilon}$  equation was found to yield slightly better results and is more convenient for computer processing. Maximum error with  $\bar{\epsilon}$  equation was 58% and minimum error was 3% with the average error over 11 separate tests being 24%. These results were better than those obtained with the Ackers-White Transport Formula which is one of the better formulae. Further tests of this hydrographic method are recommended.

## RÉSUMÉ

Une étude expérimentale a été effectuée dans un canal d'étude des sédiments pour examiner l'utilité de déterminer le charriage de fond en utilisant la hauteur du lit et la vitesse obtenue à partir des séquences des profils du lit mobile à des intervalles connus. À cette fin, une analyse théorique a été faite pour obtenir une équation générale du charriage de fond. Elle a démontré qu'il fallait un coefficient pour tenir compte à la fois de la géométrie du lit et de la partie du lit qui contribue au transport du charriage de fond. Une analyse dimensionnelle a indiqué que le coefficient devrait varier selon les conditions de l'écoulement. Un examen des données déjà publiées a démontré qu'un tel coefficient varie beaucoup selon le chiffre de mobilité et semble indépendant de la profondeur, à toutes fins utiles.

Aux fins d'application aux données touchant les profils de fond, l'équation générale du charriage de fond a été adaptée à deux cas spéciaux et mise à l'épreuve. Dans la première équation, on a utilisé une hauteur de lit  $\bar{y}$  obtenue en divisant le volume par unité de largeur des lits par leur longueur. Dans la seconde équation, on a utilisé l'écart moyen autour de l'élévation moyenne du lit comme hauteur caractéristique du lit. On a constaté que l'équation  $\bar{e}$  donnait des résultats légèrement meilleurs et convenait davantage au traitement des données par ordinateur. Le taux maximal d'erreur, dans les cas où l'on a utilisé l'équation  $\bar{e}$ , a été de 58 p. cent, et le taux minimal a été de 3 p. cent, tandis que le taux moyen a été de 24 p. cent dans l'exécution de 11 tests distincts. Ces résultats sont supérieurs à ceux que l'on a obtenus à l'aide de la méthode d'Ackers et de White, qui est très bonne. Il est recommandé de mettre davantage à l'épreuve cette méthode hydrographique.

Knowledge of the erosion and deposition of sediment relative to land surfaces, streams, reservoirs and other bodies of water is important to those involved in the development and management of water and land resources. The complex phenomena of fluvial processes make the required measurements and related data analysis expensive in comparison with other hydrologic data. To obtain knowledge of sediment movement in streams, it is necessary to determine suspended and bed-load transport over a wide range of hydraulic conditions. Whereas the suspended load can often be determined with sufficient accuracy by direct measurement, this is not the case for bed-load. Present methods such as the use of bed-load samplers (Stichling 1969), and tracer techniques (Nelson, Coakley 1974) are as yet too imprecise, time consuming and costly for general application in large rivers.

In the absence of a feasible field measurement technique, workers in fluvial hydraulics are confounded by a variety of possible formulae for computing sediment transport from measured flow parameters (Yalin 1972, Raudkivi 1976). Transport over long periods of time is usually deduced from recordings of river stage through stage-discharge relations and water flow-sediment transport relationships. The highly sensitive response of bed-load discharge to water flow (i.e. increase in stage) makes this approach very suspect (Crickmore 1967). In addition, the indirect computations of bed-load transport through measured flow parameters may give highly erroneous results because this method does not take into account availability of sediment.

The limitations of the available bed-load formulae make it clear that, at present, direct measurements in the field are still a requirement. The limitations of existing sampler and tracer methods indicate that there is room for further development of measurement methodology.

In this study, it is intended to examine the method in which bed-load is computed using the movement of bed-forms. Recent advancements in echo sounding and navigational equipment have made it possible to conduct rapid profile surveys of a given river reach using fast moving survey boats (Karaki et al 1961, Wiebe 1972, Hart 1973) Figure 1.1. Surveys can be made quickly and precisely and when applied at a suitable frequency over a given traverse will provide both spatial and temporal data of the moving bed-forms. It is therefore of

interest to find out if these profiles can yield data suitable for computation of bed-load transport.

An experimental study was conducted in a sediment flume to assess the usefulness of such a hydrographic technique.



## 2.0 BED-LOAD EQUATIONS USING DATA FROM BED PROFILES

### 2.1 Theoretical Development

It has been known for some time that bed-load transport can be related to bed-form height and speed (Simons et al 1965, Williams 1967, Crickmore 1970). The downstream movement of a bed-form implies deposition of sediment on one part of its surface and erosion on another part. Considering a two-dimensional case, then with reference to Figure 2.1, the equation of continuity for the control volume may be written as

$$q_s - (q_s + \frac{\partial q_s}{\partial x} dx) = -\frac{\partial \eta}{\partial t} dx \quad \dots\dots\dots 2.1$$

which results in

$$\frac{\partial q_s}{\partial x} = -\frac{\partial \eta}{\partial t} \quad \dots\dots\dots 2.2$$

where  $\eta$  = elevation of the bed surface  
 $q_s$  = sediment transport in volume per unit time per unit width, including the voids  
 $x$  = downstream distance  
 $t$  = time

The speed  $U_w$  with which a bed-form progresses downstream determines the rate of rise and fall of the bed. If it is assumed that the bed-form shape remains constant, then a steady state exists (Yalin 1972) which can be defined by the following functional relationship (Crickmore 1970):

$$\eta = \phi(x - U_w t) \quad \dots\dots\dots 2.3$$

From Equation 2.3 one can obtain

$$\frac{\partial \eta}{\partial t} = -U_w \frac{\partial \eta}{\partial x} \quad \dots\dots\dots 2.4$$

Combining Equations 2.4 and 2.2 results in:

$$\frac{\partial q_s}{\partial x} = U_w \frac{\partial \eta}{\partial x} \quad \dots\dots\dots 2.5$$

from which

$$dq_s = U_w d\eta \quad \dots\dots\dots 2.6$$

Equation 2.6 shows that the change in the rate of transport at a point, for a fixed bed-form shape and speed, is proportional to the change in elevation at that point.

If one considers the transport at a given  $x$ , then

$$q_s = U_w \int_{\eta_o}^{\eta} d\eta \quad \dots\dots\dots 2.7$$

where:  $\eta_o$  = elevation of zero transport (see Figure 2.2). Integration of equation 2.7 yields

$$q_s = U_w (\eta - \eta_o) \quad \dots\dots\dots 2.8$$

The time-averaged transport over a full bed-form can be obtained by summing the transport over one wave length according to

$$\bar{q}_s \Lambda = \frac{1}{\Lambda} U_w \int_0^{\Lambda} (\eta - \eta_o) dx \quad \dots\dots\dots 2.9$$

where:  $\Lambda$  = wave length of one bed-form  
 $\bar{q}_s \Lambda$  = average transport over the bed-form,

If the profile of a river reach contains a sufficient number of bed-forms in series, then the average mass sediment transport may be expressed as

$$\bar{q}_s = U_w (\bar{\eta} - \eta_o) \quad \dots\dots\dots 2.10$$

where:  $\bar{q}_s$  = average transport per unit width over the reach  
 $(\bar{\eta} - \eta_o)$  = average value of  $(\eta - \eta_o)$  over the reach.

The rate of sediment transport is more conveniently expressed as submerged weight of the sediment since this can be directly measured during experiments. This can be written as

$$G_s = (1-p) \gamma_s U_w (\overline{\eta - \eta_o}) \quad \text{..... 2.11}$$

where:  $p$  = porosity of the sediment  
 $\overline{G}_s$  = bed-load in submerged weight/sec/unit width  
 $\gamma_s$  = submerged unit weight of sediment

Equation 2.11 shows that the transport of the bed-load corresponds to the product of the bed-form speed and the average thickness of the sediment layer above a base elevation  $\eta_o$  of zero transport.

The precise elevation of  $\eta_o$  is not normally known and is, in practice, difficult to determine and hence it is necessary to characterize the thickness of moving bed-load in terms of more measurable quantities.

The commonly used bed-form height in the literature has been the distance between the crest and the lowest point in the trough denoted by  $\Delta$ . However, to use  $\Delta$  with Equation 2.11, it is necessary to introduce two coefficients, one to account for the use of the trough elevation as datum and the other to account for the shape of the dunes. That is, one assumes that  $(\overline{\eta - \eta_o})$  can be written as

$$(\overline{\eta - \eta_o}) = k (\overline{\eta - \eta_t}) = k \alpha \Delta \quad \text{..... 2.12}$$

where:  $\eta_t$  = elevation at lowest point of trough  
 $k$  = a coefficient to correct for the use of  $\eta_t$  as datum  
 $\alpha$  = a coefficient to account for bed-form shape in the downstream direction

Upon substituting into Equation 2.11 one obtains

$$\overline{G}_s = \alpha k (1-p) \gamma_s \Delta U_w \quad \text{..... 2.13}$$

## 2.2 Determination of $(\alpha k)$ from Published Data

In order to use equation 2.13 to compute sediment transport the values for the coefficients  $\alpha$  and  $k$  have to be known. It is quite obvious that the value of  $\alpha$  can vary because it depends on the shape of the dunes. For triangular bed-forms  $\alpha=0.5$  and for sinusoidal shapes  $\alpha = 2/\pi$  (Gill 1970). Jonys (1973), in measuring dune profiles, found that the shape was convex for well developed dunes. This seems to indicate that the value of  $\alpha$  should be somewhere between  $\alpha=0.5$  and  $\alpha=2/\pi$ . Crickmore (1970) estimated a value of  $k$  by taking the theoretical profile of the back of a ripple from data by Mercer (1964) and the shape of a ripple profile in the eddy region from Raudkivi (1963) and found that  $k \approx 0.5$ .

Williams (1970) conducted experiments in which the sediment transport rate as well as dune height and speed were measured. Therefore, his data can be used to compute the value of  $(\alpha k)$  from equation 2.13. The data and the results are given in Table 2.1. The values of  $(\alpha k)$  vary between 0.165 and 1.244, thus confirming the observations by Crickmore (1970) that a constant value of  $(\alpha k)$  for all flows is not likely to suffice. For simplicity of further analysis one may now write  $K_{\Delta}=(\alpha k)$ .

## 2.3 Variation of $K_{\Delta}$ with Flow Conditions

The data of Williams have shown that  $K_{\Delta}$  varies widely for different flows. However, in order to use equation 2.13 to compute the bed-load transport, it is necessary to know  $K_{\Delta}$  a priori. Therefore, it is necessary to investigate how  $K_{\Delta}$  varies with the flow variables. This can be done by means of dimensional analysis and then inspection of available data.

The coefficient  $K_{\Delta}$  can be expressed in terms of the flow variables, characteristics of the sediment and the transporting fluid and the force of gravity. Yalin (1972) shows that gravity for water-sediment systems is most conveniently expressed implicitly in the submerged unit weight of the sediment. One may therefore write

$$K_{\Delta} = f \left[ v_*, h, \rho_g, D_{50}, \gamma_s, \theta, \beta, \rho, \nu \right] \dots\dots\dots 2.14$$

in which:  $v_*$  = shear velocity

$h$  = depth of flow

$\rho_g$  = density of sand grains

$D_{50}$  = median diameter of sand grains

$\theta$  = size distribution factor

- $\beta$  = shape factor for sand grains  
 $\rho$  = density of transporting fluid  
 $\gamma_s$  = submerged unit weight of sediment  
 $\nu$  = kinematic viscosity

By dimensional analysis the number of independent terms can be reduced by three, resulting in the following equation

$$K_{\Delta} = \phi \left[ \frac{\rho \nu_*^2}{\gamma_s D_{50}}, \frac{h}{D_{50}}, \frac{\rho_g}{\rho}, \frac{g D_{50}^3}{\nu^2}, \theta, \beta \right] \dots\dots\dots 2.15$$

The data from Williams (1970) are for one sand size only and hence the two terms  $\theta$  and  $\beta$  are constant and therefore do not require special attention. In addition, the ratio  $\rho_g/\rho$  may be considered as constant for the same sand and water for all tests. For simplicity one may also write

$$E = \frac{g D_{50}^3}{\nu^2}, Y = \frac{\rho \nu_*^2}{\gamma_s D_{50}}, Z = \frac{h}{D_{50}}$$

The value of E may be considered as being constant since only one grain size was used by Williams ( $D_{50}=1.35$  mm) and temperature variations were small. Therefore, for the data in Table 2.1, the coefficient may be expressed as

$$K_{\Delta} = [Y, Z] \dots\dots\dots 2.16$$

The data of Williams (1970) was then used to compute values of  $K_{\Delta} = \bar{G}_s / (1-p) \gamma_s \Delta U_w$ ,  $Y/Y_{cr}$  and Z. Values of  $Y/Y_{cr}$  were computed instead of only Y because  $Y_{cr}$  is the critical value of Y for which sediment motion according to the Schield's curve is just beginning. For this condition of incipient motion,  $Y/Y_{cr}=1$ . The computed dimensionless parameters are given in Table 2.2

Values of  $K_{\Delta}$  were plotted as a function of  $Y/Y_{cr}$  for fixed average values of Z=67, 113 and 157 in Figure 2.3. It can be seen that for Z=67 the data exhibit a roughly definable trend. A curve was sketched to fit the data using the following criteria as an aid. Since there is no sediment motion for  $Y/Y_{cr} < 1$ , a value of  $K_{\Delta}=0$  was assumed when  $Y/Y_{cr}=1$  and the curve was made to originate at this point. Initially, the curve rises sharply and an average peak is reached when  $Y/Y_{cr} \approx 2$ . For values of  $Y/Y_{cr} > 2$ , values of  $K_{\Delta}$  decrease, initially rapidly, with the rate of decrease becoming less as  $Y/Y_{cr}$  increases.

For values of Z=113 and 157 the values of  $K_{\Delta}$  are very scattered. There is no noticeable separation of the data for these two depths. It is therefore possible that  $K_{\Delta}$  becomes less dependent on depth as it increases to produce values of Z greater than say 100. If one assumes that a single curve

describes the data for  $Z=113$  and  $157$  then this might be approximated as shown in Figure 23.

The data of Williams (1970) extends only to values of  $Y/Y_{cr} \approx 6$ . Yalin (1972) has shown that dunes exist for values of  $Y/Y_{cr}$  as high as 65 when  $Z > 100$  and Reynolds number  $v_* D_{50}/\nu > 25$ . It is not known how  $K_\Delta$  might behave for values of  $Y/Y_{cr} > 6$ , although Figure 2.3 seems to indicate a slowly decaying value of  $K_\Delta$  with increase in  $Y/Y_{cr}$ .

#### 2.4 Summary of Data Analysis

The analysis shows that there is considerable scatter in the results when computing bed-load from measurements of bed-form height  $\Delta$  and speed  $U_w$ . Since the data reflect steady state conditions, then the most reliable measurement is that of the trapped sediment. The variance in the computed bed-load must then be due to the joint variance of  $\Delta$  and  $U_w$ . Yalin (1964) states that such scatter is due to the subjectiveness in measuring the independent variables as well as the stochastic nature of the sediment transporting process.

The analysis further shows that  $K_\Delta$  is not a constant as has usually been assumed, although the data only permit a qualitative indication of its variation with flow conditions. Instead  $K_\Delta$  appears to vary considerably for very low values of flow strength (i.e.  $Y/Y_{cr} \lesssim 2-3$ ) and this variation appears to decrease as  $Y/Y_{cr}$  increases with  $K_\Delta$  slowly decreasing. It is not clear from these data how  $K_\Delta$  varies with depth for a given value of  $Y/Y_{cr}$ . However, it appears that the variance of  $K_\Delta$  increases considerably as depth of flow increases. This is probably again due to the variance in measurements of  $\Delta$  and  $U_w$ . It is also possible that  $K_\Delta$  becomes independent of  $Z$  as this becomes greater than say 100.

The conclusions from the above observations are that measurements of bed-form height and bed-form speed should be made which permit averaging of a large number of observations in order to reduce sampling error. The Hydrographic method of obtaining a sequence of river bed profiles over the same traverse was considered to be one method of providing a large enough data sample for averaging of the pertinent variables.

Two effective bed-form heights were selected which could be computed from the bed-form profile records obtained from hydrographic surveys. These two parameters were then used together with Equation 2.11 to provide two bed-load equations for testing with the data from experiments conducted in this study. These equations are developed in section 2.5.

## 2.5 Proposed Bed Load Equations Using Alternate Bedform Heights

### 2.5.1 Equation using mean bed-form height

A departure from using  $\Delta$  as the characteristic bed-form height is the use of the profile area  $A_p$  and dividing it by the profile length  $L_p$ . Both of these variables are schematically defined in Figure 2.4 (a).

The mean height for one bed-form may thus be expressed as

$$\Psi = \frac{A_p}{L_p} \quad \text{..... 2.17}$$

By averaging over a series of bed-forms ( $L_p \gg \lambda$ ) one may also write

$$(\overline{\eta} - \eta_0) = K_\Psi \bar{\Psi} \quad \text{..... 2.18}$$

where:  $\bar{\Psi}$  = the mean bed-form height obtained from a series of bed-forms.

Substituting Equation 2.18 into Equation 2.11, the desired equation is

$$\bar{G}_s = K_\Psi (1-p) \gamma_s U_w \bar{\Psi} \quad \text{..... 2.19}$$

### 2.5.2 Equation using departures about mean bed elevation

For practical application it would be more convenient to compute a representative bed-form height with reference to the average bed elevation  $\bar{\eta}$  as the datum. This eliminates the need for making subjective judgements in selecting bed-forms from a record or values of  $\eta_t$  (elevation of the lowest point in the trough). Crickmore (1970) suggested taking the absolute departures  $\epsilon$  about  $\bar{\eta}$  and these variables are defined in Figure 2.4 (b). The average of these departures may be introduced into Equation 2.11 by writing

$$(\overline{\eta} - \eta_0) = K_\epsilon \bar{\epsilon} \quad \text{..... 2.20}$$

in which:  $\bar{\epsilon} = 1 / \sum_{i=1}^n \epsilon_i$

$$\epsilon_i = | \eta_i - \bar{\eta} |$$

$K_\epsilon$  = a coefficient

$n$  = number of departures computed.

The bed-load may then be computed from

$$\bar{G}_s = K_\epsilon (1-p) \gamma_s U_w \bar{\epsilon} \quad \text{..... 2.21}$$

Both the  $\bar{\Psi}$  and  $\bar{\epsilon}$  equations use a form of active sediment thickness which should be the average of many observations obtained from river bed profiles.



### 3.0 EXPERIMENTAL EQUIPMENT

#### 3.1 The Sediment Flume

The experimental runs for this study were made in a tilting flume, rectangular in cross section, two meters wide with glass side walls 3/4 meters high and having an overall length of about 22 meters, Figure 3.1 (a). The flume can be tilted to slopes of  $\pm 1\%$ .

Water was fed from a large constant head tank through a 16" I.D. pipe which was terminated by a diffuser in the head box of the flume. In addition, baffles were placed in the head box to ensure a satisfactory velocity distribution through the cross section of the flow at the entrance of the flume. Sediment was introduced into the flow from a gravity feed hopper located above the entrance section of the flume, Figure 3.1 (b). The feed rate could be very accurately controlled by using a rotating grooved shaft installed at the bottom of the hopper which was driven by a variable speed motor. Although the sediment was fed in a completely dry condition, it was assumed to be thoroughly wetted upon entrance to the flume. The channel floor was recessed 20 cm below the lip of the head box floor to permit placement of a "permanent" sand bed.

The water level in the flume was controlled by a set of vertical louvres at the downstream end of the flume, Figure 3.1 (a). The flow leaving the flume was split into three streams each of which flowed into a separate sediment trap. The two outside traps were used to collect sediment before steady state conditions were achieved while the centre trap was kept closed by means of a pneumatically controlled gate. Once steady state was achieved, the centre trap was also opened to begin collection of sediment for weighing. This manipulation of the sediment traps did not interfere with the set up flow conditions in the flume.

At the end of a run the sediment traps were hoisted simultaneously with a large hoisting frame and the collected sediment was removed manually. After weighing and collection of samples for grain-size analysis, the sand was dried and sieved in a small batch plant which is also located in the sediment laboratory and was then returned to the feed hopper at the head of the flume by means of over-head screw conveyor for the next run.

The sediment flume is equipped with a self propelled instrument carriage, Figure 3.1 (c), which can travel along the length of the flume on rails fastened to the laboratory floor. This carriage was used for making profile traverses of the mobile bed as well as for levelling the sand bed prior to a new run.

## 3.2 Instruments

To measure the profiles an adjustable instrument rack was used which was mounted on the upstream face of the carriage to a hand operated traverse mechanism that permits movement laterally across the full width of the flume. The rack is adjustable up and down for easy setting of probe heights. The bed level and water level probes were mounted on this instrument rack.

### 3.2.1 Bed level probe

The bed level probe is an electro-optical bed level sensor. As sediment builds up under the probe, a high impedance voltage appears in one of the circuits. In a second circuit, a large negative voltage occurs which is passed on to a power amplifier. The amplifier supplies the motor which drives the mechanism that lifts the probe away from the sediment until equilibrium is restored. The system reacts very quickly to even large elevation changes so there is little danger of damaging the probe. As the motor turns, it also activates a potentiometer, producing a signal which is used to produce an analogue record of the bed profile. The bed profile probe is shown in Figure 3.2.

### 3.2.2 Water level probe

Water surface profiles are measured by a probe that makes contact with the water surface, using the water as a conductor and thus completing a circuit. The probe and supporting rod form one arm of an A. C. bridge and a potentiometer forms another. When the probe is moved from an equilibrium position an A. C. signal is generated which is amplified and sent to the motor which drives the probe. The motor moves the probe and turns a potentiometer until the system is once again in equilibrium. The signal from the potentiometer is used to produce an analogue record of the water surface profile. The water level probe is also shown in Figure 3.2.

### 3.2.3 Longitudinal (X-AXIS) displacement indicator

Displacement along the length of the flume is measured by a large aluminum wheel whose circumference is 1/10 of the overall length of the flume. It is attached to the instrument carriage and travels on the same rails. The wheel turns a potentiometer which provides a signal that activates the pen carriage on a 'XXX' recorder. This makes it possible to repeat bed profiles over exactly the

same traverse, thereby ensuring changes in elevations are always observed at the same fixed points. A precision voltage source operating at 36.36 volts provides the power for the potentiometer.

#### 3.2.4 Analogue recorder

A Honeywell XYY' Model 540 TM recorder was used to record the signals received from the measuring wheel and the two profile probes. It produces an XY (displacement vs water level elevation) and an XY' (displacement vs bed level elevation) plot on Cartesian Coordinates on 28 x 42 cm graph paper.

#### 3.2.5 Timers

Elapsed time was measured using a precision scientific electric digital stop watch. It could be read to 1/10 of a second and was able to accumulate up to 10,000 seconds.

#### 3.3 Sand

The river wash sand used for the experiments in this study was fairly uniform in size with a median sieve diameter of 1.10 mm, Figure 3.3. Transported sediment collected in the traps had virtually the same size distribution as the material remaining on the flume bed. Most of the grains were not particularly spherical and their edges were of intermediate roundness. The specific gravity of the sand was found to be 2.65 and its porosity was on the average 0.45.

#### 4.0 EXPERIMENTAL PROCEDURE AND PRELIMINARY DATA ANALYSIS

##### 4.1 Initial Considerations

Under the restrictions of a specific flume, a specific transporting fluid and a specific sediment and when mean values of the variables are obtained for equilibrium condition, one may write

$$\phi ( Q, G_s, S, h ) = 0 \quad \text{..... 4.1}$$

where:  $Q$  = fluid discharge  
 $S$  = energy slope

Williams (1967) found that as soon as depth was chosen as an independent variable, the interrelationships between  $Q$ ,  $S$  and  $G_s$  were uniquely defined. Brooks (1958), Laursen (1958), Kennedy and Brooks (1965) and Stein (1965) found that if discharge  $Q$  and depth  $h$  were chosen then both  $G_s$  and  $S$  are uniquely determined. Although there are several combinations, whenever the slope  $S$  is chosen as a controlled (independent) variable, then the other variables are not uniquely determined (Rathburn et al, 1969). For the present study, therefore, experiments were conducted by taking the discharge  $Q$  and the depth  $h$  as the independent variables.

##### 4.2 Initiations of Runs and Attainment of Equilibrium

The experiments were divided into runs and traverses. A run was a test for a specific flow condition and consisted of a series of traverses (profiles) a specific length of time apart.

To begin a run the flume was set at a slope which was expected to be close to the final equilibrium slope. This often reduced the time required to reach steady state conditions. Water was then passed very slowly over the carefully levelled sand bed with tail louvres closed until a depth of 60 cm was reached. The louvres were then gradually opened, the flow increased and the sediment feed started. Adjustments in depth, flow and sediment feed were continued until the flow was close to the desired depth. The sediment feed was carefully watched to ensure that there would be minimal aggrading or degrading of the over-all mobile bed.

When the flow was at or close to the required depth after dunes had formed, test profiles of the water surface and the bed were made to see if any changes were occurring. Attempts were made to compare the slopes of the water surface and bed profile to see if they were parallel, but this turned out to be too impractical. The bed was too irregular due to the presence of dunes and as a result the slope obtained for the bed had a large variance. Consequently, only the water surface slope was used as an indicator of steady state conditions. If water surface profiles taken from 1/2 to several hours apart showed no appreciable change in slope and if on the average the sediment bed looked uniform and there was no visual evidence of aggrading or degrading, then the water-sediment system was considered to be in equilibrium and the flow taken as being uniform. It usually took about 24 hours of continuous running to achieve this steady state condition. Once this condition was achieved, measurements were begun to obtain the necessary data.

#### 4.3 Experimental Measurements

The measurements actually made during the experiments were the water surface profiles and bed profiles, water discharge and sediment discharge.

##### 4.3.1 Measurement of profiles

The profiles were measured over a working section nine metres in length, the upstream end of which was located nine metres below the flume entrance. All profiles were initiated at the beginning of the working section ( $x=0$  on 'YYY' recorder) and taken on the centre-line of the flume. At the start of the first traverse the digital stop watch was started and kept running during the entire run thereby providing a continuous, cumulative time record. At the end of each profile, the time was noted while the carriage stopped automatically. The carriage was then returned to its starting position. At the start of the next traverse, the accumulated time was noted and the same procedure followed as before. The run was usually completed when 20 or more traverses had been taken.

##### 4.3.2 Measurement of water discharge

The water discharge was obtained by measuring the overflow from the constant head tank which supplies the flume. The overflow was trapped in a carefully calibrated volumetric tank over a suitable length of time, thus permitting the computation of the overflow rate. The flow in the flume was then

simply the difference between the rate of inflow into the constant head tank from the pump and the overflow. This method allowed an accuracy of better than 3%. The discharges are given in Table 4.1

#### 4.3.3 Measurement of sediment discharge

The sediment transport was collected in the trap from the time at which steady state conditions were achieved to the end of the run which, on the average, was about 12 hours. The sediment was withdrawn from the trap and placed into a  $3/4 \text{ m} \times 3/4 \text{ m} \times 1 \text{ m}$  steel box suspended from a monorail hoist. The box was then submerged in water and the submerged sediment weight obtained with a dynamometer, Figure 4.1, which was accurate within 0.5 kg. This process was repeated until all the sand was weighed. The total sediment discharge rate was computed by dividing the weighed sand by the total elapsed time in seconds and is given in Table 4.1.

#### 4.4 Interpretation of the Profiles

The water surface and bed profiles recorded on the 'XYY' recorder were digitized and the data stored on electromagnetic tape. A computer program was written to make linear interpolations between successive digitized values to convert the profile records into discrete, elevation points a fixed distance apart. This made it possible to compare all elevations for different profiles at the same points along the length of the profiles. There were 9000 such points, 1 mm apart, for each profile record.

##### 4.4.1 Water surface slope

The treated data was fed into a computer program to compute the water surface slope by linear regression. This was repeated for each traverse in a given run. The slope for the run was then simply the arithmetic average of the slopes for the individual traverses. The slope for each run together with the standard deviation is given in Table 4.1.

##### 4.4.2 Depth of flow

The water depth was obtained by taking the differences in elevations at the interpolated even intervals along the profiles between the water surface and the bed elevations. The average depth for a traverse was then the arithmetic average of all the differences taken. The overall average for a run was simply the average depth for all the traverses in that run. These are given together with

their standard deviation in Table 4.1. The water depth was an independent variable and as such its value was set. In all cases, the coefficient of variation for the depth in a given run was less than 7%.

#### 4.4.3 Bed-form speed

Since the rate of profiling is much faster than the rate of bed-form propagation downstream, each point on a profile may be considered as being an instantaneous picture of the stream bed taken at some time  $t_j$ . Hence the sequence of successive profiles represents a time series for each point on the profiles with time increments.

$$\Delta t_j = t_{j+1} - t_j \quad \dots\dots\dots 4.2$$

where  $t_{j+1}$  = instantaneous time at which the  $(j+1)$ th profile is taken  
 $t_j$  = as above for the  $j^{\text{th}}$  profile.

The time increment  $\Delta t_j$  must be chosen so that the advancement of the bed-forms during this period is not so great as to permit sufficient profile shape distortion, thereby preventing an adequate measurement of dune displacement. On the other hand,  $\Delta t_j$  must not be so short as to render too small a value of bed-form displacement for reasonable measurement. For this study in the sediment flume,  $\Delta t_j$  was taken to be from three to five minutes.

The average velocity of the bed-forms was computed by cross correlation of successive profiles (traverses) according to the relationship

$$R(\ell) = \frac{\sum_{i=1}^n y_j(X_i) \cdot y_{j+1}(X_i + \ell)}{n - 2} \quad \dots\dots\dots 4.3$$

where:  $R(\ell)$  = coefficient of cross-correlation at lag between the  $j^{\text{th}}$  and  $(j+1)^{\text{th}}$  profile.

$y_j(X_i)$  = elevation at the  $i^{\text{th}}$  point in the  $j^{\text{th}}$  profile with zero mean and unit variance.

$\ell$  = relative longitudinal displacement (lag) between  $j^{\text{th}}$  and  $(j+1)^{\text{th}}$  profile.

$n$  = number of points observed

Cross-correlations were performed for different values of the lag  $\ell$  and the value of  $\ell$  for the maximum value of  $R(\ell)$  was taken as the average displacement of bed-forms during the time  $\Delta t_j$  between successive profiles. The average bed-form speed was then computed from

$$\bar{U}_w = \frac{\bar{\ell}}{\Delta t_j} \quad \dots\dots\dots 4.4$$

where:  $\bar{\ell}$  = average displacement of bed-forms.

The average bed-form speed for a given run was then taken as the average of the speeds obtained from successive traverses. The speed for each run together with its standard deviation is given in Table 4.1.

#### 4.4.4 Bed-form heights

##### 4.4.4.1 Mean bed-form height $\bar{\psi}$

To determine the mean height  $\psi$ , bed-form areas were defined by drawing straight line segments between troughs and successive bed-forms, Figure 2.4 (a). Partial bed-forms at the ends of the records were not included. The boundaries of the bed-form areas were then digitized and the areas computed. The mean height  $\psi$  was then taken to be the arithmetic average of the bed-form areas  $A_i$  divided by the length of profile subtending this area. These heights were obtained for each traverse and their overall average was taken to be the mean height  $\bar{\psi}$  for a given run. Values of  $\bar{\psi}$  together with their standard deviation are given in Table 4.1.

##### 4.4.4.2 Average departure about mean elevation, $\bar{\epsilon}$

The mean elevation  $\bar{\eta}$  was computed for each traverse by simply averaging all the discrete elevations over the length of a given profile. The departures  $\epsilon_i$  were computed at each discrete point and the average departure taken as the arithmetic mean of the absolute values of all the individual departures. The overall average departure  $\bar{\epsilon}$  for a run was then simply the average of the values obtained for all the traverses in the run. The values of  $\bar{\epsilon}$  and their standard deviation are given in Table 4.1.



## 5.0 ANALYSIS OF THE PROPOSED BED-LOAD EQUATIONS

### 5.1 The $\bar{\Psi}$ Equation

Values of  $K_{\Psi}$  were computed from Equation 2.19 using the measured values of  $G_s$ ,  $U_w$  and  $\bar{\Psi}$  obtained from the bed profiles. These were plotted as a function of  $Y/Y_{cr}$  in Figure 5.1 (a).

The values of  $K_{\Psi}$  are over a range of  $3 < Y/Y_{cr} < 6$ . Over the same range of  $Y/Y_{cr}$ , it was observed in Figure 2.3 that  $K_{\Delta}$  appeared to be decreasing as the value of  $Y/Y_{cr}$  increased. The data for  $K_{\Psi}$ , however, is too limited to discern such a trend. The data are for average values of  $Z = 120, 150$  and  $185$  but there was no discernable effect due to depth. A similar observation was made for  $K_{\Delta}$  when  $Z$  was greater than  $100$ .

Since there was no discernable trend in the plotted data, the average value of  $K_{\Psi}$  was computed and found to be  $\bar{K}_{\Psi} = 0.70$  for an average flow strength of  $(\bar{Y}/Y_{cr}) \approx 4$ , using all the data regardless of the depth. For a value of  $(\bar{Y}/Y_{cr}) \approx 4$ , the average value of  $K_{\Delta}$  was  $K_{\Delta} = 0.52$ . It was expected, based on geometric considerations only that  $\bar{K}_{\Psi} \approx 2\bar{K}_{\Delta}$  since  $\bar{\Psi} \approx 2\Delta$ . However, other factors such as smaller grain-size used in determining  $\bar{K}_{\Psi}$  and the large degree of variance in the small data sets may account for the fact that  $\bar{K}_{\Psi} \lesssim 2K_{\Delta}$ . It must also be remembered that the value of  $\bar{K}_{\Psi} = 0.70$  is only tentative over the narrow range of  $Y/Y_{cr}$  given in Figure 5.1(a). Since it was shown that  $K_{\Delta}$  varies with  $Y/Y_{cr}$  then  $K_{\Psi}$  can be expected to vary in a similar way. However, more data are required to define values of  $K_{\Psi}$  over a wider range of  $Y/Y_{cr}$ .

The percent deviations of  $K_{\Psi}$  about the average  $\bar{K}_{\Psi} = 0.70$  were then computed and these are shown in Table 5.1.

The percent deviation varied between 49.6% and -42.2%. The absolute average deviation was 28.2% with a standard deviation of 13.4%. This indicated that errors can be considerable when using the  $\bar{\Psi}$  equation to compute bed-load.

### 5.2 The $\bar{\epsilon}$ Equation

Values of  $K_{\epsilon}$  were computed from Equation 2.21 using the measured values of  $G_s$ , as well as  $U_w$  and  $\bar{\epsilon}$  obtained from the bed profiles. These were plotted in Figure 5.1 (b).

The values of  $K_{\epsilon}$  are over the same range of  $Y/Y_{cr}$  as those for  $K_{\Psi}$ . Similar to the observations for  $K_{\Psi}$ , there was considerable scatter in the  $K_{\epsilon}$  values and there was no evidence of any depth effects.

Since there was no noticeable trend in the plotted data, the average value of  $K_\epsilon$  was computed and found to be  $\bar{K}_\epsilon = 1.17$ , for an average value of flow strength of  $(\bar{Y}/Y_{cr}) \approx 4$ . Crickmore (1970) found very good agreement between measured and computed bed-load when  $Y/Y_{cr} \approx 4$  by using a value of  $K_\epsilon = 1.32$ , which is within 13% of  $\bar{K}_\epsilon = 1.17$ . The difference in the two values of the coefficient may be due to the fact that for the tests of Crickmore (1970) a sand with  $D_{50}$  of 0.66 mm was used, whereas the sand used for the present tests had a  $D_{50}$  of 1.1 mm. Therefore, the value of  $\bar{K}_\epsilon = 1.17$  seems to be reasonable. However, it must again be emphasized that this value of  $K_\epsilon$  is only tentative over the narrow range of flow strength  $3 < Y/Y_{cr} < 6$ . It is considered most likely that similar to the case of  $K_\Delta$ ,  $K_\psi$ ,  $K_\epsilon$  must vary significantly with  $Y/Y_{cr}$ , especially for values of  $Y/Y_{cr} < 3$ .

The percent deviations of the  $K_\epsilon$  values about the average  $\bar{K}_\epsilon = 1.17$  were then computed and these are shown in Table 5.2. The percent deviations vary between 57.8% and -33.0%. The absolute average deviation was 24.1% with a standard deviation of 17.1%. These results indicate that on the average the  $\bar{\epsilon}$  equation is only slightly better than the  $\bar{\psi}$  equation for computing bed-load. This observation is contrary to what had been expected. It was felt that by using the departures  $\epsilon$  the entire information content of the profiles would be used while at the same time avoiding subjective judgements in selecting individual bed-forms as is the case in determining  $\bar{\psi}$ .

### 5.3 Comparison Between the Proposed Bed-load Equations and the Ackers-White Sediment Transport Formula

The hydraulic data and median sand size from the present study were applied to the Ackers-White (1973) formula. Comparisons were then made by using the percent errors obtained with Ackers-White formula and the percent deviations about the two average coefficients  $\bar{K}_\psi$  and  $\bar{K}_\epsilon$ . The Ackers-White formula was chosen because it is perhaps the most reliable formula over a wide range of flow conditions and has been found suitable also when dunes were the dominant bed-form (Bayazit, 1974). This formula utilizes the advantages of dimensional analysis but the basic form of the equation is based on theoretical arguments. It is not proposed to discuss the Ackers-White formula in detail but some basic explanations are given to indicate the general principles.

The formula is an extension of the original theory developed by Bagnold (1966). The general transport function is given in dimensionless form as

$$G_g = f_1 \left[ F_g, E_g \right] \quad \dots\dots\dots 5.1$$

where:  $G_g$  = dimensionless sediment transport rate  
 $F_g$  = mobility number  
 $E_g$  = dimensionless diameter of grains

The dimensionless transport, mobility number and dimensionless grain diameter are defined by the equations

$$G_g = \frac{x}{s} \cdot \frac{h}{D_{50}} \left[ \frac{v_*}{V} \right]^n \quad \dots\dots\dots 5.2$$

$$F_g = \frac{v_*^n}{\sqrt{g(s-1) D_{50}}} \left[ \frac{v}{\sqrt{32 \log \frac{\alpha h}{D_{50}}}} \right]^{1-n} \quad \dots\dots\dots 5.3$$

and

$$E_g = D_{50} \left[ \frac{g(s-1)}{v^2} \right]^{\frac{1}{3}} \quad \dots\dots\dots 5.4$$

where:  $V$  = average velocity of flow  
 $s$  = specific gravity  
 $\alpha$  = a coefficient  
 $x$  = concentration of sediment.  
 $n$  = an exponent

For values of  $E_g < 1$  (very fine sediment)  $n=0$  and for  $E_g > 60$  (very coarse sediment)  $n=1$ . The median grain-size for this study was  $D_{50}=1.1$  mm, which results in a value of  $E_g \approx 27$  defined by Ackers and White to be in the transitional range of  $1 < E_g < 60$ . For this transitional case the general transport function may be written as

$$G_g = C \left[ \frac{F_g}{F_{gcr}} - 1 \right]^m \quad \dots\dots\dots 5.5$$

where:  $F_{gcr}$  = value of  $F_g$  at nominal initial sediment motion  
 $C$  = a coefficient  
 $m$  = an exponent

It was found that  $F_{gcr}$ ,  $C$ ,  $m$  and  $n$  would all vary with sediment size parameter  $E_g$ . Values of  $F_{gcr}$ ,  $C$ ,  $m$  and  $n$  as a function of  $E_g$  were obtained by optimization of best fit relationships given by

$$n = 1.00 - 0.56 \log E_g \quad \dots\dots\dots 5.6$$

$$F_{gcr} = \frac{0.23}{\sqrt{E_g}} + 0.14 \quad \dots\dots\dots 5.7$$

$$m = \frac{9.66}{E_g} + 1.34 \quad \dots\dots\dots 5.8$$

$$\log C = 2.86 \log E_g - (\log E_g)^2 - 3.53 \quad \dots\dots\dots 5.9$$

The data from the present study were used to compute the values of  $n$ ,  $F_{gcr}$ ,  $m$  and  $C$ . The bed-load  $G_s$  could then be computed once values of  $x$  and  $G_g$  were determined.

The percent deviations between computed and measured bed-load were then obtained and these are shown in Table 5.3. The maximum percent deviations varied from -64% to +61.7%. The absolute average deviation was 36.9% with a standard deviation of 19.1%. These results indicate that errors obtained with the Ackers-White formula are likely to be greater than those obtained with the  $\bar{\Psi}$  and  $\bar{\epsilon}$  equations. Moreover, the formula tended to underestimate the measured bed-load in most cases.

The considerable variance in determining the bed-load from measurements of bed-forms and the use of hydraulic variables in a sediment transport formula, attest to the fact that accurate values of bed-load are very difficult to obtain. Indeed, it is probably not possible to measure bed-load much more precisely than indicated by this study. One will probably have to be content with errors which on the average would appear to be of the order of 25% to 35%. The

bed-load transport in the dune regime is a very stochastic process which in actuality is three-dimensional, but is usually measured in the two-dimensional sense. Measurements with samplers yield errors which are often much greater than those indicated here.

The  $\bar{\epsilon}$  equation had the lowest average percent error. This equation although only marginally better than the  $\bar{\Psi}$  equation is more readily applicable for computer computation. It, therefore, appears that the  $\bar{\epsilon}$  equation together with measurements of  $\epsilon$  and  $U_w$  may be useful if more about the behaviour of the coefficient  $K_\epsilon$  can be learned from further experiments. An equation such as this has the advantage over conventional bed-load formulae in that it allows computation of bed-load from data obtained by measuring the actual movement of sediment. These measurements can be done on a large river in about three hours with presently available equipment.

## 6.0 CONCLUSIONS

- 6.1 Examination of published data indicate that the method of computing bed-load using maximum bed-form height and speed as independent variables, requires a coefficient  $K_{\Delta}$  which is dependent on rate of flow.
- 6.2 The variation of the coefficient  $K_{\Delta}$  is non-linear being most sensitive at lower values of  $Y/Y_{cr}$ . The results further indicate that the coefficient may be independent of depth when values of  $h/D_{50} > 100$ . Under these conditions the coefficient appears to increase for values of  $Y/Y_{cr}$  up to 2-3, and decrease thereafter. More data is required to further assess the behaviour of the coefficient.
- 6.3 The coefficients  $K_{\Psi}$  and  $K_{\epsilon}$  appear to be also independent of depth for  $h/D_{50} > 100$ . It is considered most probable that these coefficients will vary with  $Y/Y_{cr}$  in a way similar to  $K_{\Delta}$ .
- 6.4 The error in computing bed-load with the  $\bar{\epsilon}$  equation is on the average slightly lower than that obtained with the  $\bar{\Psi}$  equation. The  $\bar{\epsilon}$  equation is also more suitable than the  $\bar{\Psi}$  equation because it is more readily adapted for computer processing and requires no subjective judgement in determining the bed-form height.
- 6.5 The use of the hydrographic method with the  $\bar{\epsilon}$  equation has the advantage of measuring actual moving sediment simultaneously over a series of bed forms. Therefore, it is likely to be more accurate than measurements with samplers over an equal period of sampling time.
- 6.6 The Ackers-White formula, which can be regarded as one of the more reliable formula available, does not predict bed-load any more accurately than the  $\bar{\epsilon}$  equation.
- 6.7 The study results indicate that it is probably not possible to measure bed-load with errors less than 25% to 35% because of the stochastic nature of the transport process. In view of this, the hydrographic method using the  $\bar{\epsilon}$  equation can be a useful tool once the coefficient  $K_{\epsilon}$  is better defined. Therefore, tests over a wider range of  $Y/Y_{cr}$  should be made.
- 6.8 Other methods for computing bed-load ought to be investigated.

### ACKNOWLEDGEMENTS

All the measurements and photographs were made by Mr. F. Dunnette who also set up the instrumentation with the assistance of Mr. D. Fekyt. All computer programs were written and made operational by Mrs. K. Beal and for her diligence the writer is especially grateful.

The writer also wishes to express his gratitude to Dr. Y. L. Lau, Head, Hydraulics Section and Dr. B. G. Krishnappan for their assistance during the preparation of this study.

## REFERENCES

- Ackers, P. and White, W. R., 1973. "Sediment Transport: New Approach and Analysis". American Society of Civil Engineers, Journal of the Hydraulics Division, Vol. 99, No. 11.
- Bagnold, R. A., 1966. "An Approach to the Sediment Transport Problem from General Physics". Professional Paper 4221 U.S. Geological Survey, Washington, D. C.
- Bayazit, M., 1974. "Sediment Transport: New Approach and Analysis". Discussion, American Society of Civil Engineers, Journal of the Hydraulics Division, Vol. 100, No. HY9.
- Brooks, N. H., 1958. "Mechanics of Streams with Moveable Beds of Fine Sand". American Society of Civil Engineers Trans., Vol. 123, pp 526-549.
- Crickmore, M. J., 1967. "Measurement of Sand Transport in Rivers with Special Reference to Tracer Methods". Sedimentology, Vol. 8, No. 3.
- Crickmore, M. J., 1970. "Effect of Flume Width on Bedform Characteristics". American Society of Civil Engineers, Journal of the Hydraulics Division, Vol. 96, No. HY2.
- Gill, M. A., 1971. "Height of Sand Dunes in Open Channel Flow". American Society of Civil Engineers, Journal of the Hydraulics Division, Vol. 97, No. HY12.
- Hart, E. D., 1973. "Schoaling Measurements in Navigable Waters by the U. S. Army Corps of Engineers". International Symposium on River Mechanics, Bangkok, Thailand.
- Jonys, C. K., 1973. "An Experimental Study of Bed-Form Mechanics". Thesis in Partial Fulfillment of the Requirements for the Degree of Doctor of Philosophy, Dept. of Civil Engineering, University of Alberta, Canada.
- Karaki et al, 1961. "Dual Channel Stream Monitor". American Society of Civil Engineers, Journal of the Hydraulics Division, Vol. 87, No. HY6.
- Kennedy, J. F. and Brooks, N. H., 1965. "Laboratory Study of an Alluvial Stream at Constant Discharge". Proceedings of Federal Inter-Agency Sediment Conference, U. S. Department of Agriculture Misc. Pub. 970, pp 320-330.
- Laursen, E. M., 1958. "The Total Sediment Load of Streams". American Society of Civil Engineers, Journal of Hydraulics Division, Vol. 84, No. HY1.
- Mercer, A. G., 1964. "Characteristics of Sand Ripples in Low Froude Number Flow". Thesis submitted to the University of Minnesota in Partial Fulfillment of the Requirements for the Degree of Doctor of Philosophy.



- Nelson, D. E. and Coakley, J. P., 1974. "Techniques for Tracing Sediment Movement". Scientific Series No. 32., Inland Waters Directorate, Canada Centre for Inland Waters, Burlington, Ontario.
- Rathburn, R. E. and Guy, H. P., 1967. "Measurement of Hydraulics and Sediment Transport Variables in a Small Recirculating Flume". Water Resources Research, Vol. 3, No. 1.
- Raudkivi, A. J., 1963. "Loose Boundary Hydraulics". 1st ed. Pergamon Press, Oxford.
- Raudkivi, A. J., 1976. "Loose Boundary Hydraulics". 2nd ed. Pergamon Press, Oxford.
- Simons et al, 1965. "Bedload Equation for Ripples and Dunes". Geological Survey Professional Paper 462-H, Washington, D. C., U.S.A.
- Stichling, W., 1969. "Instrumentation and Techniques in Sediment Surveying". Proceedings of Hydrology Symposium No. 7, National Research Council of Canada Associate Committee on Geodesy and Geophysics, Subcommittee on Hydrology, Victoria, B. C. 14-15 May.
- Stein, R. A., 1965. "Laboratory Studies of Total Load and Apparent Bedload". Journal of Geophys. Research, Vol. 70, No. 8, pp 1831-1842.
- Wiebe, K., 1972. "A Description of the Hydac-100 System and its Application". Sediment Survey Section, Applied Hydrology Division, Dept. of Fisheries and Environment, Ottawa.
- Williams, G. P., 1967. "Flume Experiments on the Transport of a Coarse Sand". Geological Survey Professional Paper 562-B, Washington, D. C. U.S.A.
- Williams, G. P., 1970. "Flume Width and Water Depth Effects in Sediment Transport Experiments". Geological Survey Professional Paper 562-H, Washington, D. C., U.S.A.
- Yalin, M. S., 1964. "Geometrical Properties of Sand Waves". American Society of Civil Engineers, Journal of the Hydraulics Division, Vol. 90, No. HY5.
- Yalin, M. S., 1972. "Mechanics of Sediment Transport". Pergamon Press, Toronto.

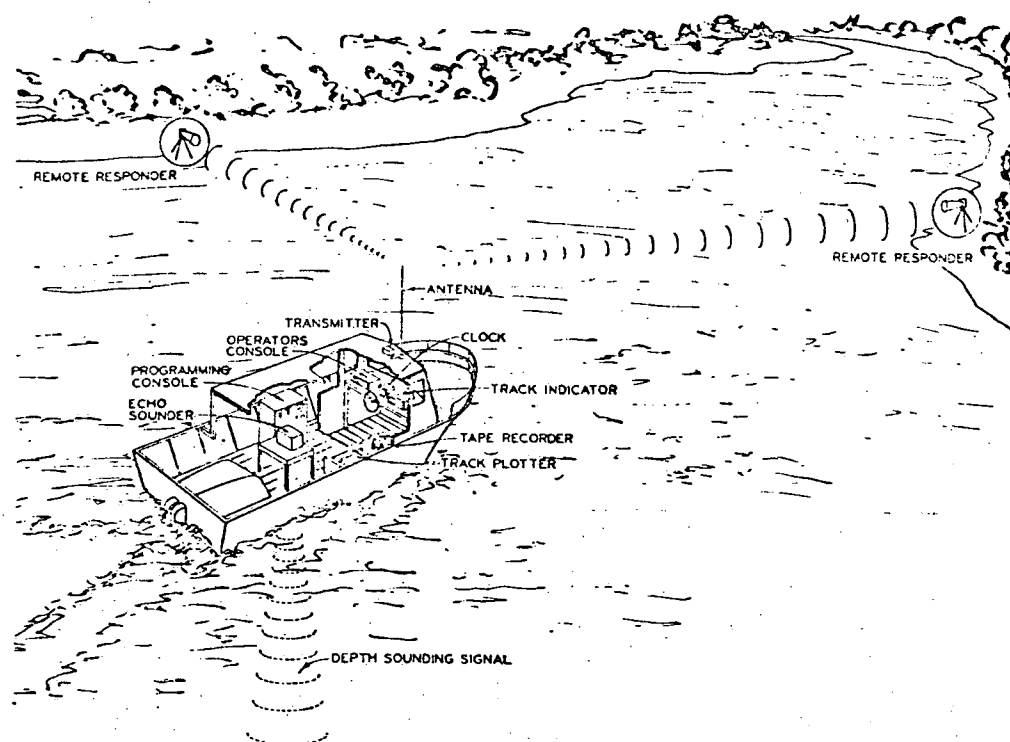


FIGURE 1.1 DATA COLLECTING HYDROGRAPHIC SURVEY  
BOAT (After HART 1973)

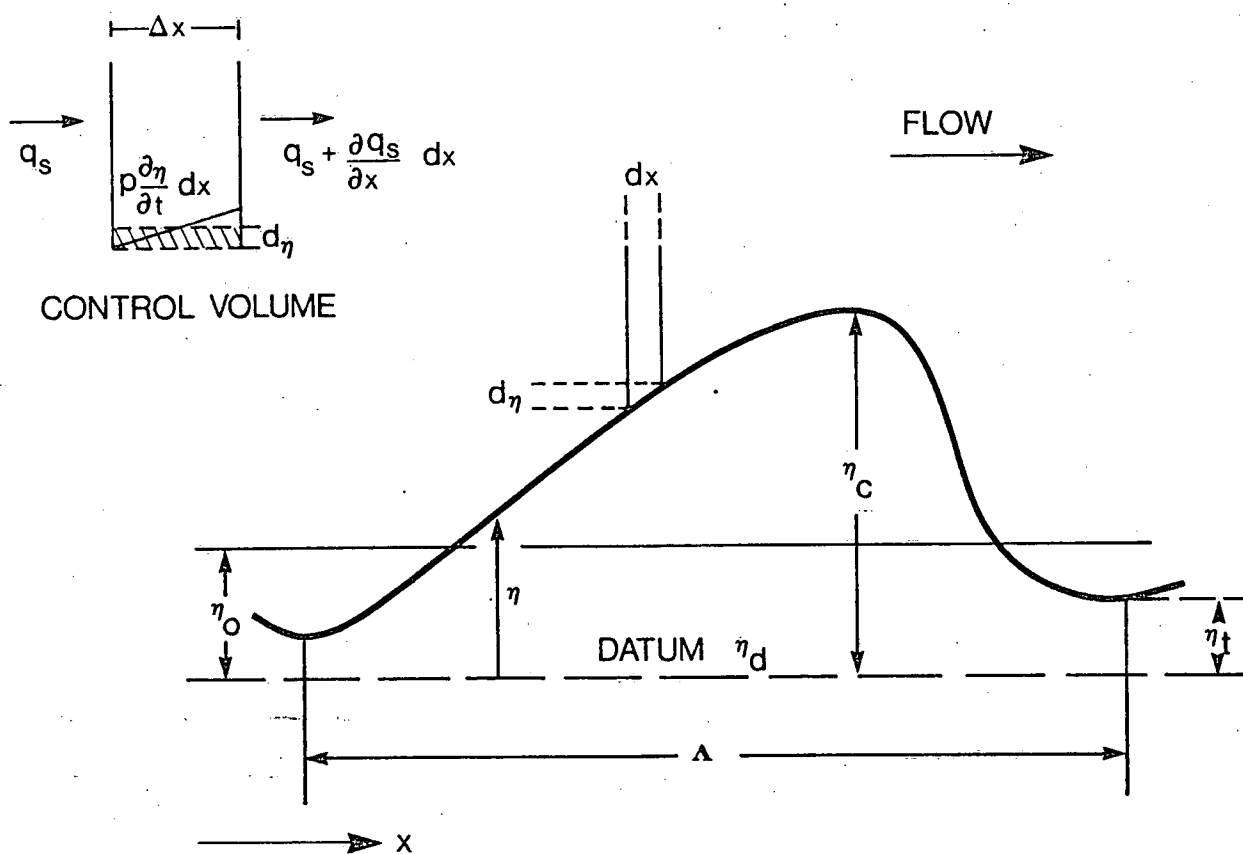


FIGURE 2.1 DUNE PROFILE DEFINITION SKETCH

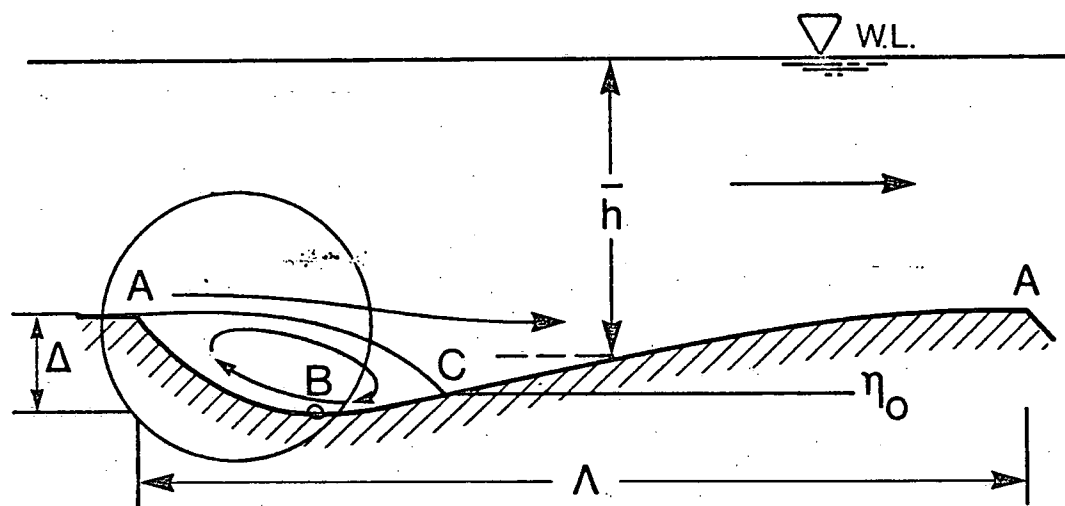


FIGURE 2.2 ELEVATION OF ZERO TRANSPORT.  $\eta_0$   
(after Yalin, 1964)

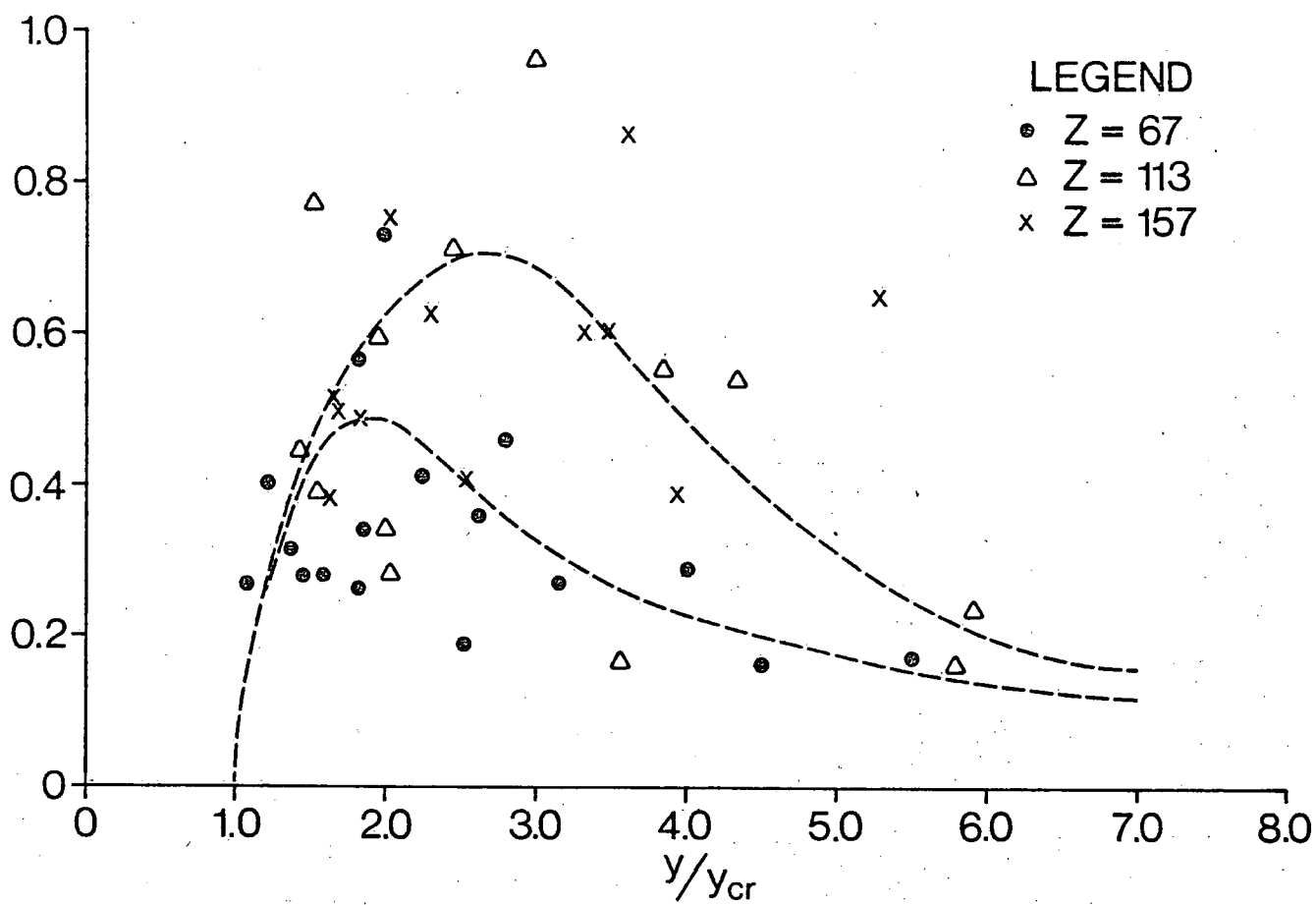


FIGURE 2.3 VARIATION OF  $K_\Delta$  WITH FLOW STRENGTH

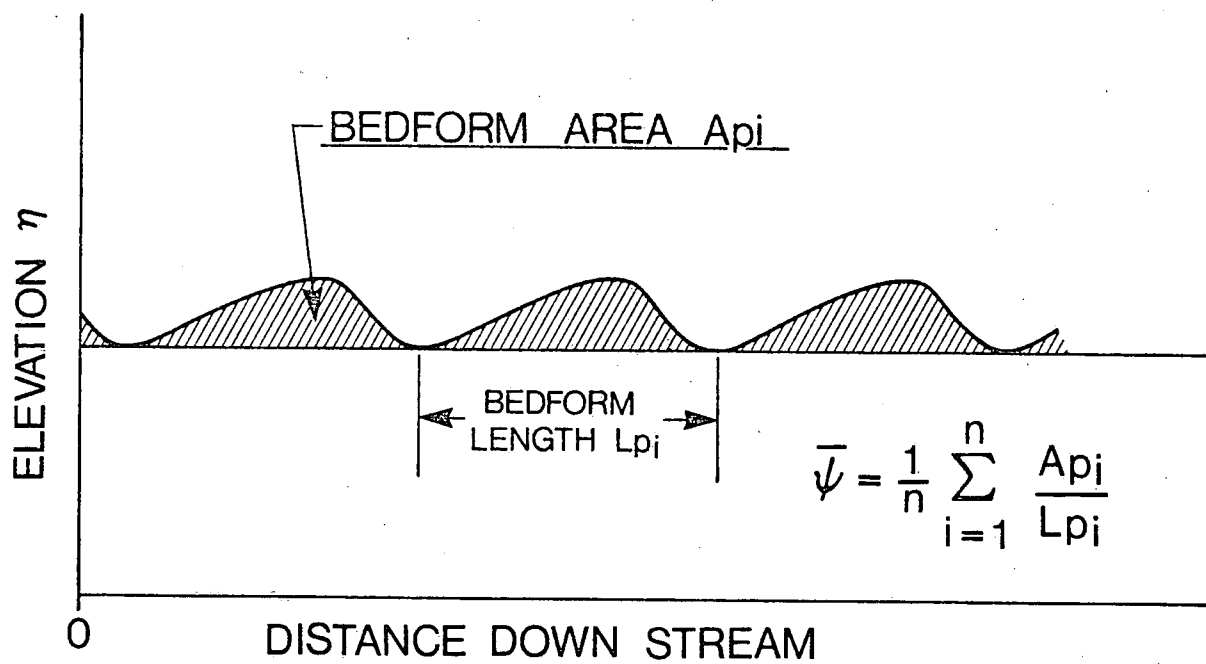


FIGURE 2.4(a) DEFINITION OF BEDFORM HEIGHT  $\bar{\psi}$

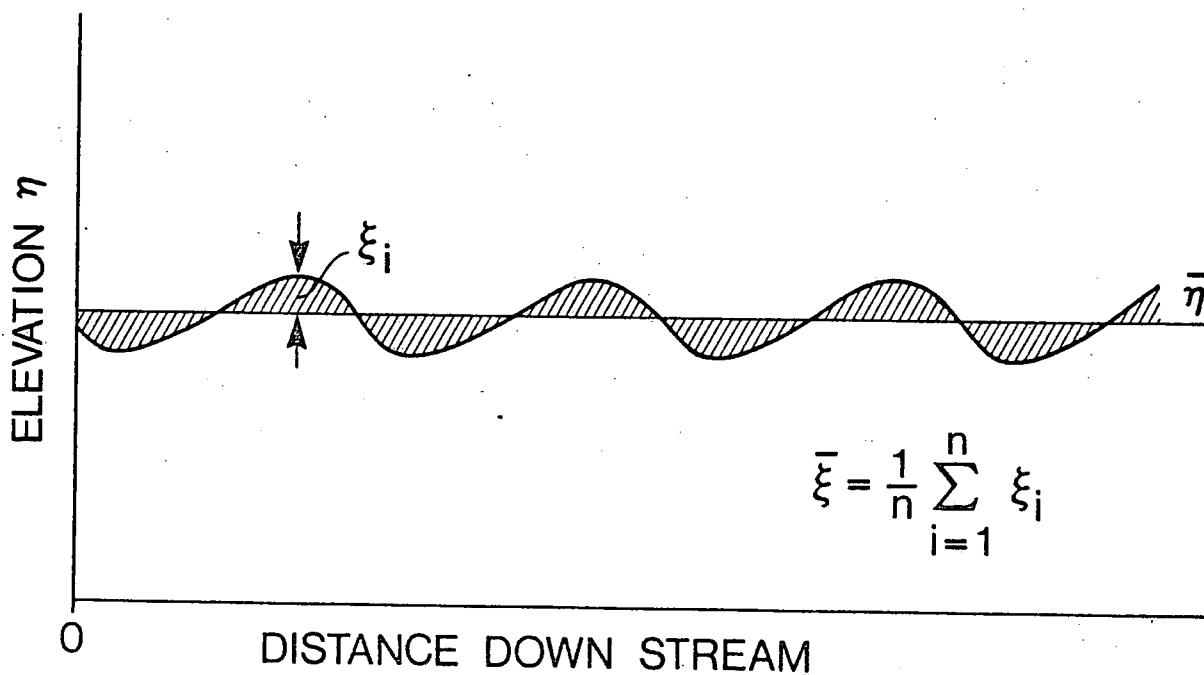


FIGURE 2.4 (b) DEFINITION OF BEDFORM HEIGHT  $\bar{\xi}$

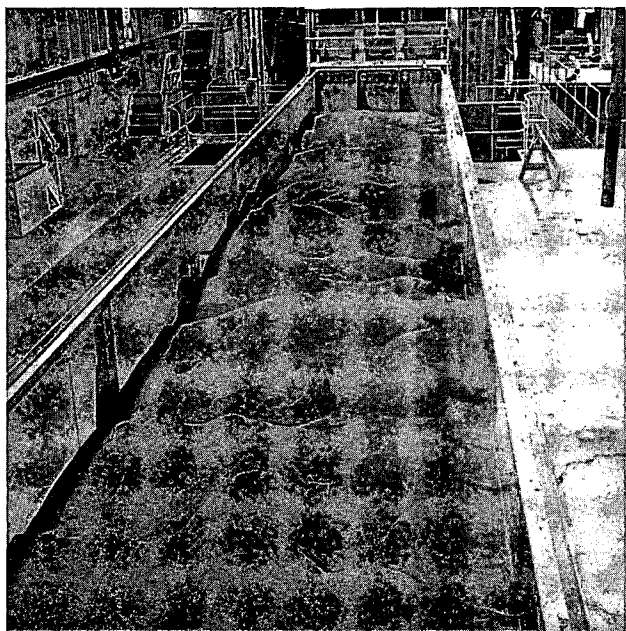


FIGURE 3.1(a) 2m FLUME

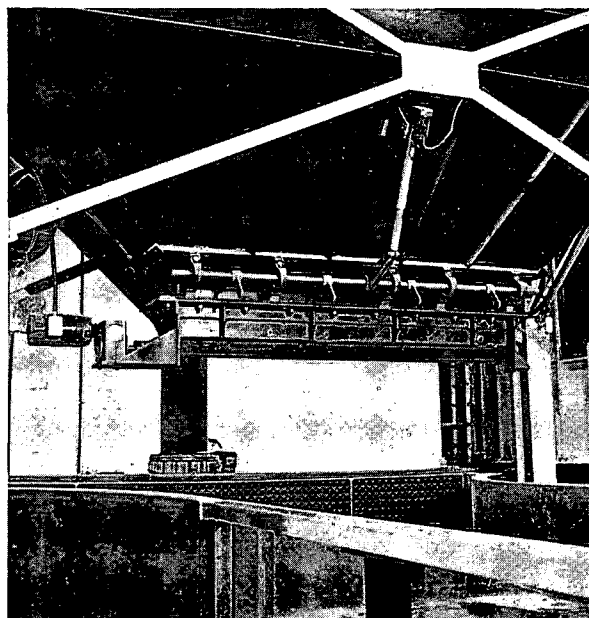


FIGURE 3.1(b) FEED HOPPER

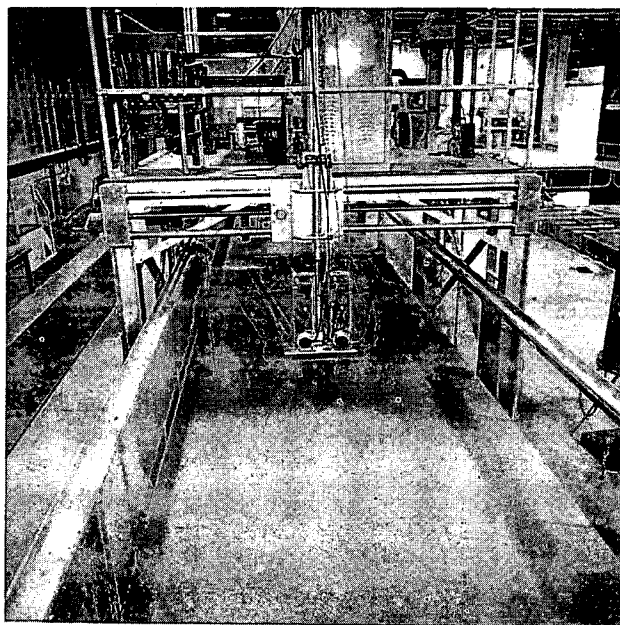


FIGURE 3.1 (c) INSTRUMENT CARRIAGE

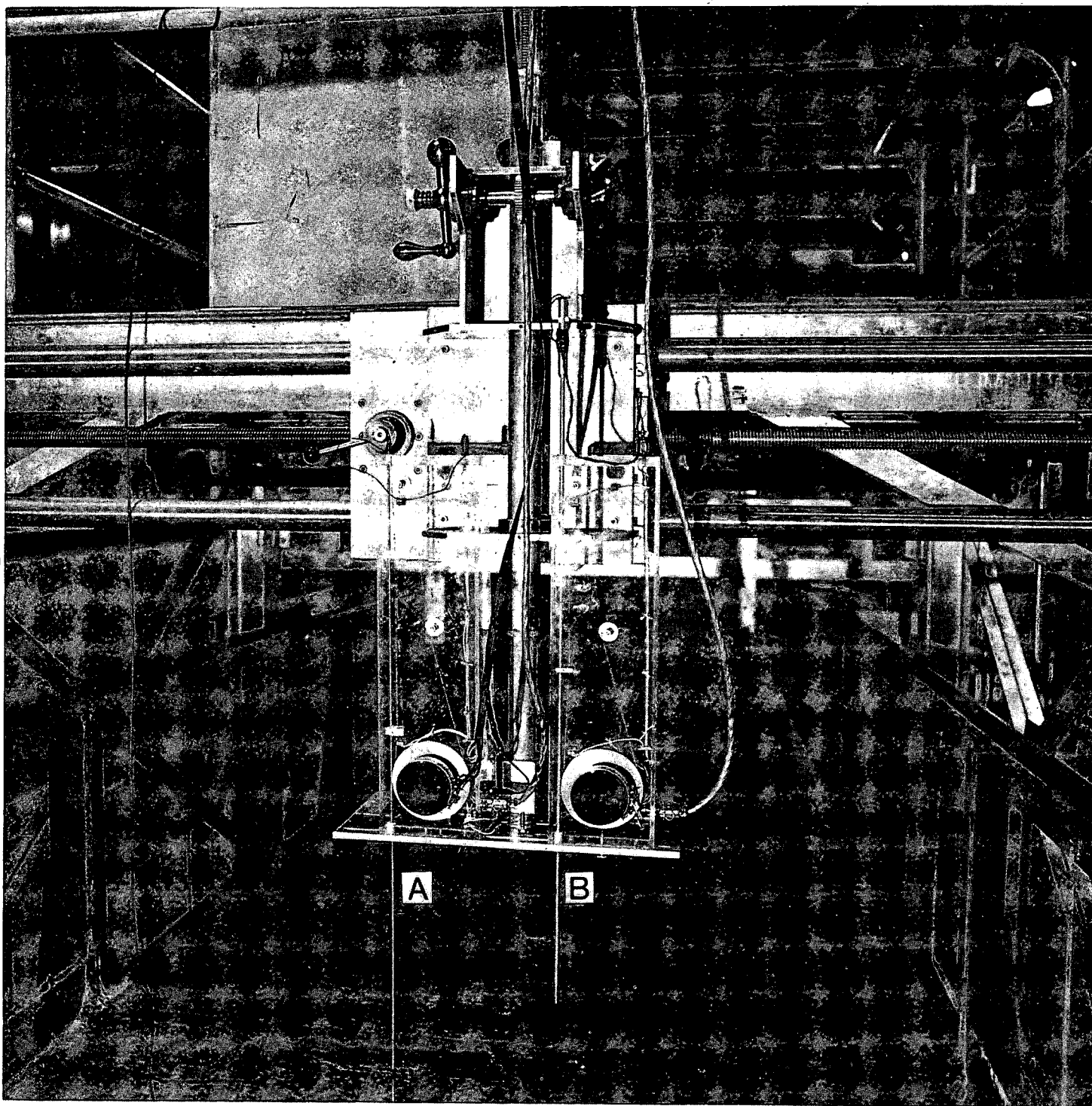


FIGURE 3.2 WATER LEVEL PROBE (A) AND BED LEVEL PROBE (B)



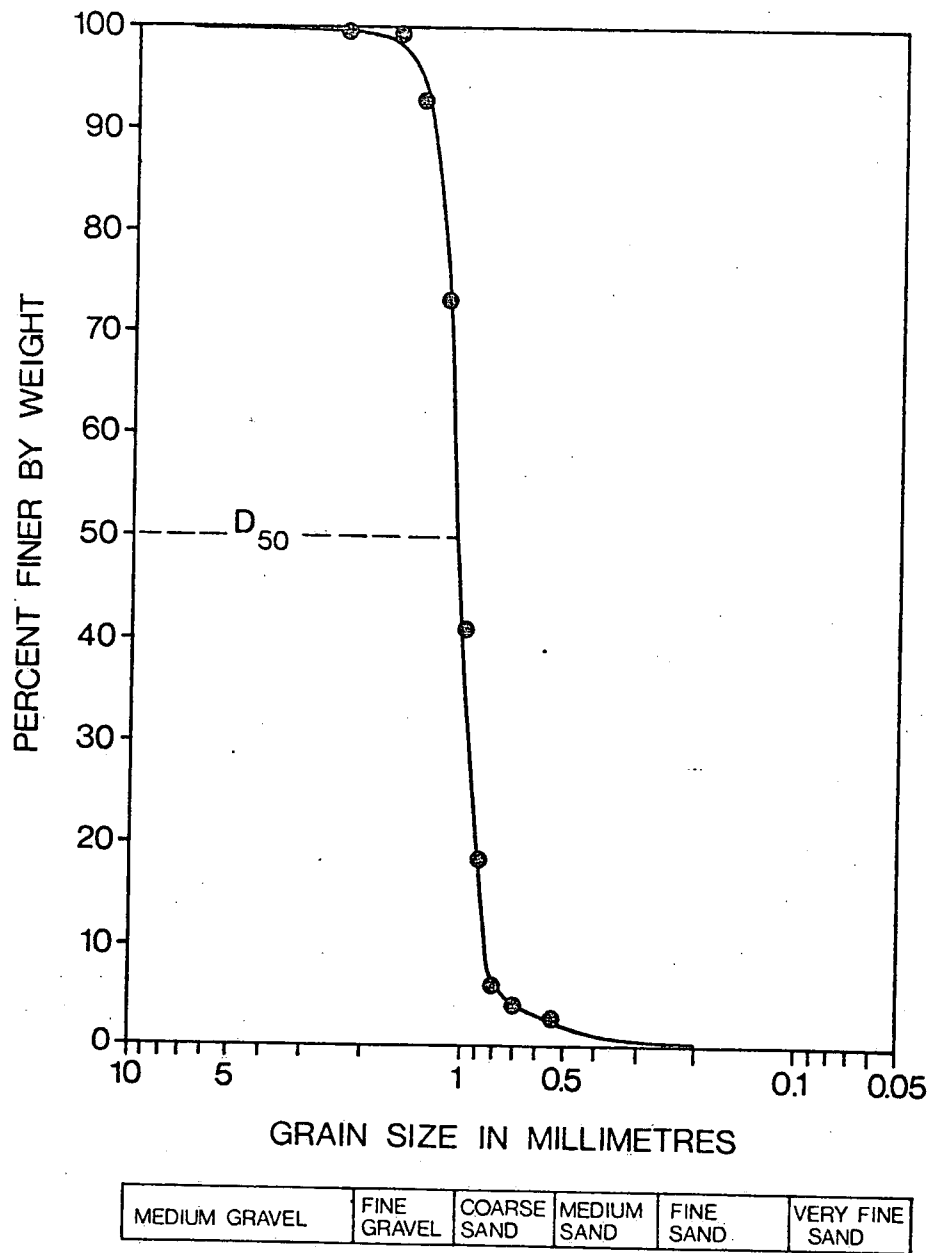


FIGURE 3.3 GRAINSIZE DISTRIBUTION OF TEST SAND

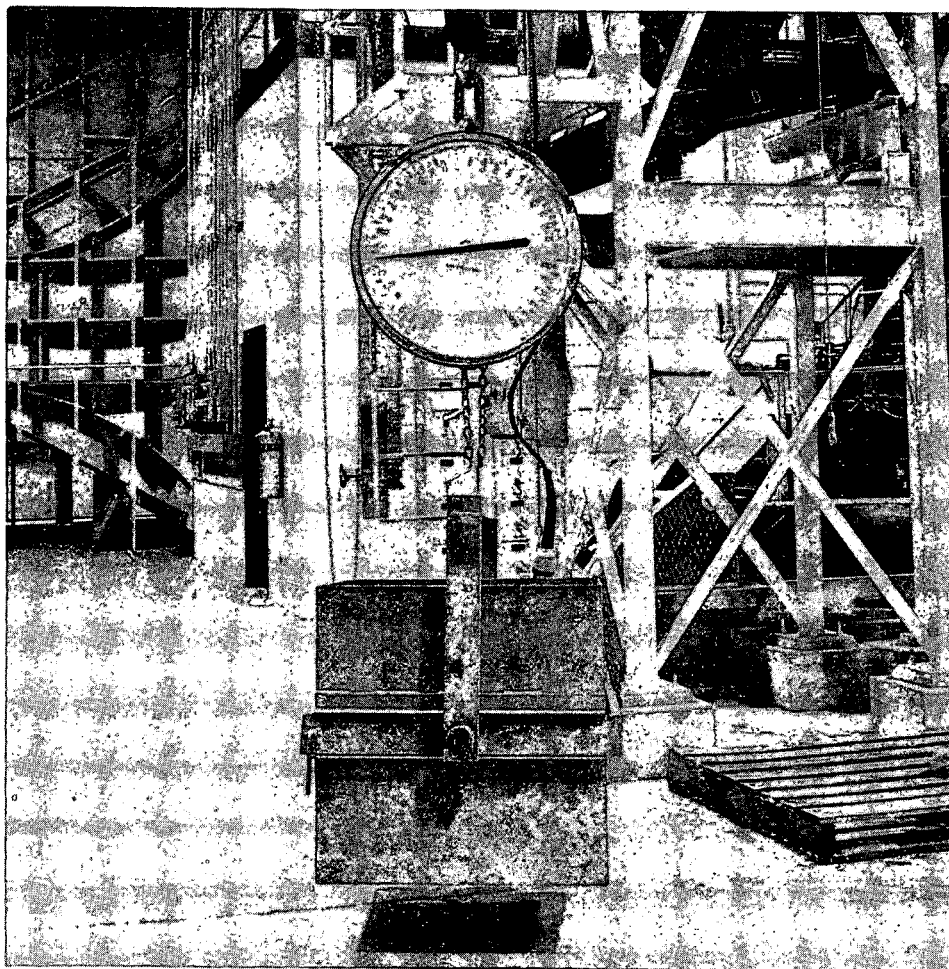


FIGURE 4.1 DYNAMOMETER FOR WEIGHING SAND

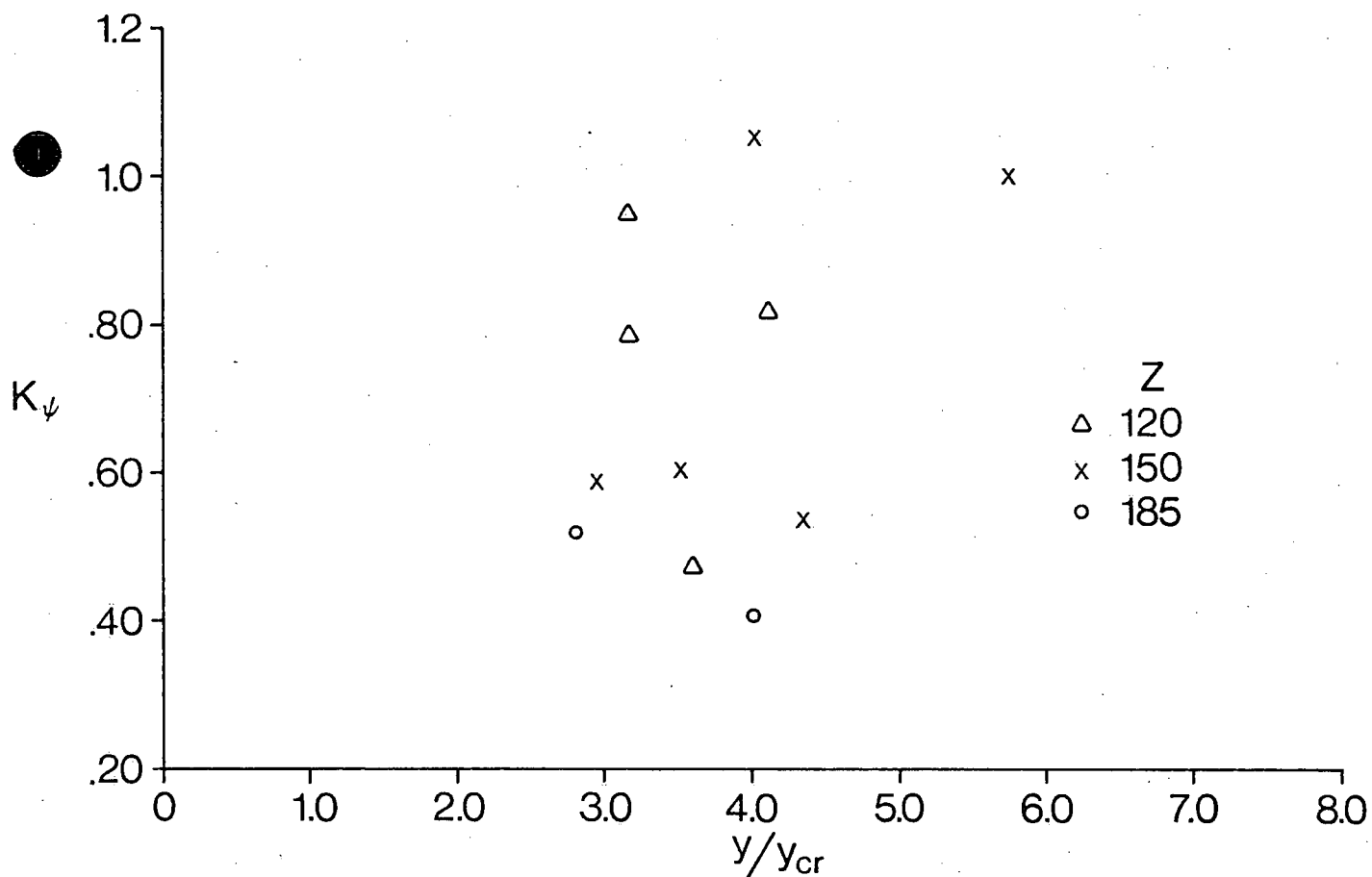


FIGURE 5.1(a) VARIATION  $K_\psi$  WITH MOBILITY NUMBER

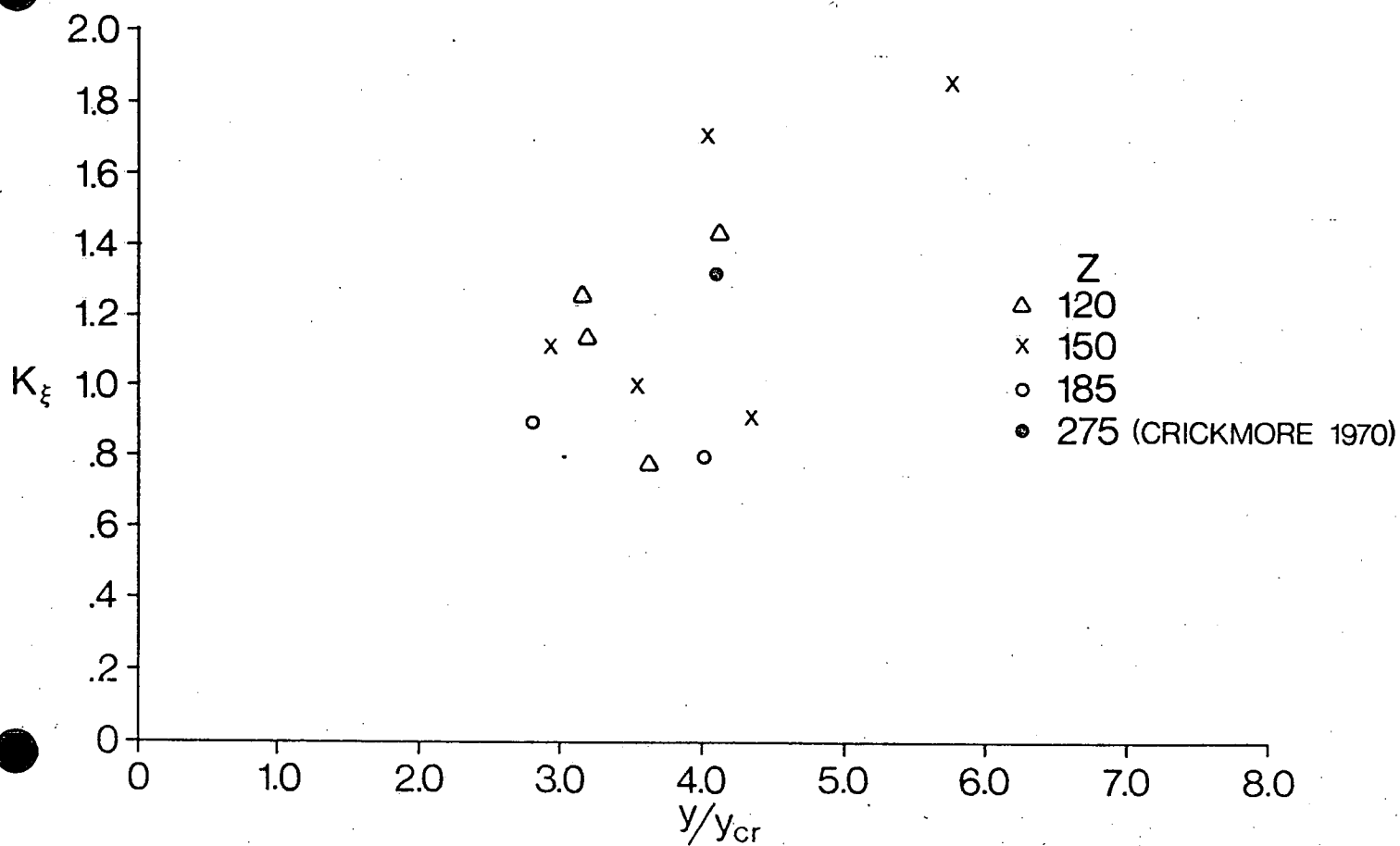


FIGURE 5.1(b) VARIATION OF  $K_\xi$  WITH MOBILITY NUMBER

TABLE 2.1  
PUBLISHED DATA FROM WILLIAMS (1970)

RUN	h m	q <sub>w</sub> l/s/m	G <sub>s</sub> Kg/s/m	S	U <sub>w</sub>	Δ m	αk
107	.096	40.8	.000461	.00121	.00021	.006	.403
109	.090	40.6	.00159	.00162	.00052	.012	.281
110	.090	42.0	.00254	.00182	.00082	.012	.284
111	.091	43.6	.00381	.00200	.00046	.016	.570
112	.092	46.2	.00537	.00210	.00110	.020	.269
113	.093	46.8	.00558	.00211	.0015	.012	.342
114	.090	47.6	.00870	.00236	.00082	.016	.731
115	.090	49.2	.0138	.00272	.0023	.016	.413
116	0.088	51.2	.0162	.00318	.0036	.026	.191
117	0.088	53.0	.0238	.00397	.0048	.020	.273
118	0.088	60.4	0.0470	.00509	.0081	.022	.291
119	0.090	68.8	.0570	.00557	.0076	.050	.166
122	.095	73.8	.0714	.00643	.0117	.038	.177
154	.087	39.8	.000997	.00118	.00040	.010	.274
155	.090	41.8	.00179	.00154	.00062	.010	.319
156	.088	46.4	.00625	.00210	.0010	.015	.459
157	.088	54.8	.0185	.00330	.0028	.020	.364
128	.153	71.4	.000646	.00106	.00013	.014	.391
129	.155	78.6	.00302	.00137	.00037	.026	.346
130	.148	73.8	.00308	.00133	.00021	.012	
131	.154	80.4	.00429	.00144	.00052	.032	.284
132	.158	84.0	.00713	.00172	.00055	.020	.714
133	.156	89.2	.00908	.00184	.00067	.012	
134	.154	89.0	.0107	.00216	.00061	.020	.966
135	.158	97.6	.0168	.00251	.0022	.050	.168
136	.154	102.2	.0293	.00314	.0019	.050	.543
137	.155	122.6	.0496	.00416	.0066	.050	.165
160	.146	72.4	.00106	.00106	.00015	.010	.778
161	.150	79.4	.00195	.00097	.00032	.015	.447
162	.152	81.8	.00454	.00137	.00042	.020	.596
163	.152	103.2	.0210	.00281	.0012	.035	.550
164	.148	119.8	.0539	.00445	.0062	.040	.239
141	.212	108.6	.000695	.00081	.000095	.016	.504
142	.217	115.2	.00213	.0079	.00023	.020	.510
143	.214	122.6	.00481	.00131	.00050	.026	.408
144	.218	132.0	.00868	.00178	.00066	.024	.604
145	.216	152.4	.0299	.00272	.0011	.046	.650
167	.211	104.0	.00870	.00060	.00015	.020	
168	.208	119.4	.00223	.00080	.00032	.020	.385
169	.216	127.2	.00610	.00147	.00020	.025	
170	.215	130.6	.0109	.00172	.00057	.035	.602
171	.215	167.2	.0440	.00280	.0012	.040	
173	.225	119.8	.00232	.00096	.00017	.020	.753
174	.215	119.0	.00305	.00091	.00017	.040	.494
175	.215	126.4	.00546	.00115	.00024	0.040	.626
176	.210	132.8	.0124	.00191	.00035	.045	.867
177	.205	136.6	.0167	.00214	.00087	.055	.385

TABLE 2.2  
DIMENSIONLESS PARAMETERS

RUN	Z	Y	Y <sub>cr</sub>	Y/Y <sub>cr</sub>	K <sub>Δ</sub>
107	71	.05225	.044	1.185	.403
108	67	.06555	.046	1.425	.281
110	67	.07354	.047	1.565	.284
111	67	.08171	.048	1.815	.570
112	68	.08673	.048	1.807	.269
113	69	.08809	.048	1.835	.342
114	67	.09535	.048	1.987	.731
115	67	.1099	.049	2.243	.413
116	65	.1256	.050	2.512	.191
117	65	.1568	.050	3.136	.273
118	65	.2011	.050	4.022	.291
119	67	.2251	.050	4.502	.166
122	70	.2742	.050	5.484	.177
154	64	.04609	.043	1.072	.274
155	67	.06222	.046	1.353	.319
156	65	.08296	.047	1.765	.459
157	65	.1304	.050	2.608	.364
128	113	.0728	.047	1.549	.391
129	115	.0953	.048	1.985	.346
130	110	.08837	.048	1.841	
131	114	.09956	.049	2.032	.284
132	117	.1220	.050	2.440	.714
133	116	.1289	.050	2.578	
134	114	.1493	.050	2.986	.966
135	117	.1780	.050	3.560	.168
136	114	.2171	.050	4.342	.543
137	115	.2895	.050	5.790	.165
160	108	.0695	.046	1.511	.778
161	111	.06532	.046	1.420	.447
162	113	.09349	.048	1.948	.596
163	113	.1918	.050	3.836	.550
164	110	.2957	.050	5.914	.239
141	157	.07709	.047	1.640	.504
142	161	.07696	.047	1.638	.510
143	159	.1259	.050	2.518	.408
144	162	.1742	.050	3.484	.604
145	160	.2638	.050	5.276	.650
167	156	.05684	.045	1.263	
168	154	.07470	.047	1.589	.385
169	160	.1426	.050	2.852	
170	159	.1660	.050	3.320	.602
171	159	.2703	.050	5.406	
173	167	.09697	.048	2.020	.753
174	159	.08783	.048	1.830	.494
175	159	.1110	.049	2.265	.626
176	156	.1801	.050	3.602	.867
177	152	.1970	.050	3.940	.385

TABLE 4.1

## EXPERIMENTAL RESULTS USING HYDROGRAPHIC METHOD

Run No.	Flow Depth		W. S. Slope		Fluid Discharge	Bedload Discharge	Mean Departures		Mean Dune Ht.		Dune Speed	
	$\bar{h}$ m	$\sigma_h$ m	S	$\sigma_s$	Q m <sup>3</sup> /s	G <sub>s</sub> K /m/sec	$\epsilon$ m	$\sigma_\epsilon$ m	$\bar{\Psi} = \frac{A_p}{L_p}$ m	$\sigma_\Psi$ m	U <sub>w</sub> m/s	$\sigma_u$ m/s
1	0.1606	0.00266	0.00184	0.00023	0.175	0.0166	0.0201	0.00193	0.03220	0.00397	0.000602	0.0001146
2	0.2010	0.00317	0.00221	0.00025	0.148	0.0232	0.0229	0.00073	0.03660	0.00679	0.000594	0.0000852
3	0.1665	0.00924	0.00237	0.00024	0.175	0.01335	0.01905	0.00240	0.03218	0.00517	0.0008452	0.0002707
4	0.1498	0.00150	0.00171	0.000119	0.150	0.00885	0.01641	0.00202	0.03077	0.00651	0.0005374	0.0000701
5	0.1544	0.00199	0.00227	0.00031	0.171	0.01770	0.01750	0.00213	0.02860	0.00253	0.0006516	0.0000906
6	0.1664	0.00256	0.00313	0.00044	0.203	0.03360	0.01846	0.00307	0.03380	0.00813	0.001087	0.0000826
7	0.1626	0.00359	0.00103	0.00008	0.164	0.01065	0.01624	0.001603	0.03310	0.00573	0.0004199	0.00005858
8	0.1417	0.00912	0.00196	0.00011	0.160	0.01545	0.02069	0.00427	0.03030	0.000565	0.0007327	0.00009376
9	0.1989	0.00434	0.00181	0.00016	0.240	0.0150	0.02367	0.00213	0.0465	0.0071	0.000877	0.00001032
10	0.2082	0.00159	0.00115	0.00012	0.253	0.00923	0.02149	0.00159	0.0374	0.0061	0.000526	0.0000646
11	0.1907	0.00417	0.00181	0.00014	0.257	0.0362	0.02687	0.00386	0.0376	0.0042	0.000739	0.0000697
12	0.17825	0.00237	0.00172	0.00013	0.218	0.0154	0.02086	0.00174	0.0348	0.0060	0.000812	0.000001
13	0.12696	0.00152	0.00206	0.00018	0.121	0.01283	0.01467	0.00093	0.02561		0.000675	0.00001094
14	0.12871	0.00331	0.00208	0.00021	0.124	0.01531	0.01792	0.00312	0.02336		0.0007789	0.00001126
15	0.13575	0.00248	0.00231	0.00020	0.138	0.0116	0.01793	0.00214	0.02947		0.0009087	0.00001400

 $\sigma$  = standard deviation

Table 5.1

DEVIATIONS OF  $K_{\Psi}$  ABOUT  $\bar{K}_{\Psi}$ 

Run No.	Z	$K_{\Psi}$	% Deviation
3	151	.540	-22.9
4	136	.590	-15.7
5	140	1.047	49.6
6	151	1.009	44.1
8	129	.776	10.9
9	181	.405	-42.2
10	189	.516	-26.3
12	162	.602	-14.0
13	115	.817	16.7
14	117	.948	35.4
15	123	.477	-31.9
		Average 0.70	Absolute Average 28.2

Table 5.2

DEVIATIONS OF  $K_{\epsilon}$  ABOUT  $\bar{K}_{\epsilon}$ 

Run No.	Z	$K_{\epsilon}$	% Deviation
3	151	.914	-21.9
4	136	1.106	- 5.5
5	140	1.702	45.5
6	151	1.846	57.8
8	129	1.136	- 2.9
9	181	.798	-31.8
10	189	.896	-23.4
12	162	1.000	-14.5
13	115	1.426	21.9
14	117	1.247	6.6
15	123	.784	-33.0
		Average 1.17	Absolute Average 24.1



Table 5.3 DEVIATIONS OF COMPUTED BED-LOAD USING ACKERS-WHITE FORMULA

Run No.	Z	$G_{sm}$ Kg/s/m	$G_{sc}$ Kg/s/m	$\left( \frac{G_{sc} - G_{sm}}{G_{sm}} \right) \times 100\%$
3	151	.0134	.0093	-30.6
4	136	.0089	.0057	-35.6
5	140	.0177	.0125	-29.4
6	151	.0336	.0233	-30.7
8	129	.0155	.0133	-14.2
9	181	.0150	.0175	16.7
10	189	.0092	.0149	61.7
12	162	.0154	.0187	21.4
13	115	.0128	.0046	-64.0
14	117	.0158	.0050	-68.4
15	123	.0116	.0077	-33.6
				Absolute Average 36.9

$G_{sm}$  = measured bed-load

$G_{sc}$  = computed bed-load

10082

